

# Effects of Shaping Conditions on the Microstructure and the Mechanical Property of the $\text{Al}_2\text{O}_3$ -YAG Eutectic Composite Produced by Melting the $\text{Al}_2\text{O}_3$ -YAP Eutectic Structure

Tomoya Nagira, Hideyuki Yasuda, Takumi Sakimura\* and Asako Kawaguchi\*

<sup>1</sup>Department of Adaptive Machine System, Osaka University, Suita 565-0871, Japan

When the  $\text{Al}_2\text{O}_3$ -YAP metastable eutectic system was heated above the metastable eutectic temperature but below the equilibrium eutectic temperature, undercooled melt was formed. Solidification in the equilibrium path accompanied the melting of the metastable eutectic system, resulting in a fine and uniform eutectic structure. A novel solidification process using undercooled melt formation was developed. In this paper, the influences of the initial  $\text{Al}_2\text{O}_3$ -YAP eutectic particle size, forming pressure and holding time at the maximum temperature on the microstructure and/or the mechanical property of the  $\text{Al}_2\text{O}_3$ -YAG compact were examined to optimize the forming conditions. The  $\text{Al}_2\text{O}_3$ -YAG compact produced from the  $\text{Al}_2\text{O}_3$ -YAP eutectic particles with diameters less than  $20\text{ }\mu\text{m}$  exhibited a higher flexural strength and the smaller porosity as compared to that produced from  $\text{Al}_2\text{O}_3$ -YAP eutectic particles with diameters ranging from  $20\text{ }\mu\text{m}$  to  $45\text{ }\mu\text{m}$ . The volume fraction of the porosity was approximately 4% under a forming pressure of 10 MPa and a holding time of 60 s. The flexural strength of the  $\text{Al}_2\text{O}_3$ -YAG compact decreased with the increase in the holding time due to the increase in the lamellar spacing. For  $\text{Al}_2\text{O}_3$ -YAP eutectic particles with diameters less than  $20\text{ }\mu\text{m}$ , a low forming pressure of 10 MPa and a short holding time of 60 s were sufficient to synthesize a dense  $\text{Al}_2\text{O}_3$ -YAG compact. Thus, the solidification technique that uses undercooled melt produced by melting the  $\text{Al}_2\text{O}_3$ -YAP metastable eutectic system has good advantages for shaping. [doi:10.2320/matertrans.MB200705]

(Received March 22, 2007; Accepted April 11, 2007; Published July 11, 2007)

**Keywords:** undercooled melt, eutectic ceramics, eutectic solidification, nucleation

## 1. Introduction

Unidirectionally solidified  $\text{Al}_2\text{O}_3$ -based eutectic ceramics have gained considerable attention as heat-resistance materials because of their superior mechanical properties at high temperatures.<sup>1-4)</sup> In recent years, Waku *et al.* reported that single crystal  $\text{Al}_2\text{O}_3$ /single crystal YAG( $\text{Y}_3\text{Al}_5\text{O}_{12}$ : yttrium-aluminum-garnet) eutectic composites exhibited a flexural strength of 360–400 MPa at temperatures ranging from room temperature to 2073 K.<sup>2-4)</sup> In addition to excellent mechanical properties at high temperatures, some interesting solidification phenomena have been reported in the  $\text{Al}_2\text{O}_3$ - $\text{Y}_2\text{O}_3$  system.<sup>5-7)</sup> Caslavsky and Viechnickl discovered the two eutectic reactions by optical differential thermal analysis in the  $\text{Al}_2\text{O}_3$ -rich part of the  $\text{Al}_2\text{O}_3$ - $\text{Y}_2\text{O}_3$  phase diagram—one is the  $\text{Al}_2\text{O}_3$ -YAG equilibrium eutectic reaction at 2099 K and the other is the  $\text{Al}_2\text{O}_3$ -YAP metastable eutectic reaction at 1975 K, as shown in Fig. 1.<sup>7)</sup>

The  $\text{Al}_2\text{O}_3$ -YAP metastable eutectic system can be selected in the composition range of 13.5–28.5 mol%  $\text{Y}_2\text{O}_3$ .<sup>7-10)</sup> When the melt that has a metastable eutectic composition is heated to temperatures above 2273 K, the  $\text{Al}_2\text{O}_3$ -YAP metastable system is indispensably selected. In our previous work,<sup>8-15)</sup> heating the  $\text{Al}_2\text{O}_3$ -YAP metastable eutectic system up to temperatures above the metastable eutectic temperature, undercooled melt for  $\text{Al}_2\text{O}_3$ -YAG equilibrium eutectic system was produced due to melting of the  $\text{Al}_2\text{O}_3$ -YAP metastable eutectic structure at the metastable eutectic temperature.

The solidification of the  $\text{Al}_2\text{O}_3$ -YAG equilibrium eutectic system accompanies the melting of the  $\text{Al}_2\text{O}_3$ -YAP metastable eutectic system. Thus, the endothermic heat generated due to melting is nearly compensated by the exothermic heat generated due to the solidification. As a result, the solid-

ification rate becomes relatively high, resulting in a fine and uniform eutectic structure. On the basis of these findings, a novel solidification technique utilizing the undercooled melt shaping has been developed.<sup>8-15)</sup>

Our previous paper demonstrated that  $\text{Al}_2\text{O}_3$ -YAG castings with a relatively complex shape were produced by the undercooled melt shaping.<sup>13)</sup> For example, the groove shape of the molybdenum mold (300  $\mu\text{m}$  in width and 1 mm in thickness) was well transferred to the castings.  $\text{Al}_2\text{O}_3$ -YAG eutectic particles with diameters in the range of 25–40  $\mu\text{m}$  were used to produce the castings. Porosities of diameters in the range of 5–10  $\mu\text{m}$  were observed in the top part of the fins. Since the  $\text{Al}_2\text{O}_3$ -YAG eutectic structure produced from undercooled melt could be influenced by the initial particle size of the  $\text{Al}_2\text{O}_3$ -YAP eutectic particles, the study of the influence of the initial particle size of the  $\text{Al}_2\text{O}_3$ -YAP on the  $\text{Al}_2\text{O}_3$ -YAG eutectic structure is of importance. In addition, it is necessary to optimize the casting conditions during the heating process in order to synthesize dense castings with a uniform microstructure.

In this paper, the influence of the initial  $\text{Al}_2\text{O}_3$ -YAP particle size, forming pressure and holding time at the maximum temperature on the  $\text{Al}_2\text{O}_3$ -YAG solidification structure and the flexural strength of  $\text{Al}_2\text{O}_3$ -YAG eutectic castings were examined in order to optimize the process conditions for undercooled melt shaping.

## 2. Experimental Procedure

$\alpha$ - $\text{Al}_2\text{O}_3$  powder (99.99%) and  $\text{Y}_2\text{O}_3$  powder (99.99%) were weighed according to  $\text{Al}_2\text{O}_3$ -23.5 mol%  $\text{Y}_2\text{O}_3$  which is an  $\text{Al}_2\text{O}_3$ -YAP metastable eutectic composition. These powders were ball milled with ethanol for 24 h to obtain homogeneous slurry that was then dried at 473 K. The mixed powder was calcined at 1573 K for 3 h in air. The calcined powder was melted in a Mo crucible by an induction furnace

\*Graduate Student, Osaka University

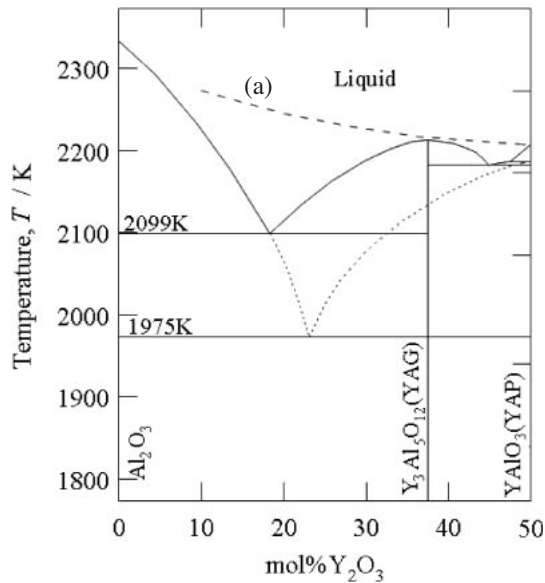


Fig. 1 Phase diagram of the  $\text{Al}_2\text{O}_3$ - $\text{Y}_2\text{O}_3$  system. The pecked lines indicate the liquidus of the metastable eutectic system. Melts cooled down from the temperatures above the dashed line (a) follow the metastable path of the solidification.<sup>7)</sup>

in vacuum. The  $\text{Al}_2\text{O}_3$ -YAP metastable eutectic structure was obtained by heating the melt to temperatures above 2300 K before solidification. The solidified specimens were crushed into particles and sieved through 45–63  $\mu\text{m}$ , 32–45  $\mu\text{m}$  and 20  $\mu\text{m}$  sieves in the decreasing order. Two kinds of  $\text{Al}_2\text{O}_3$ -YAP metastable eutectic particles with diameters less than 20  $\mu\text{m}$  and ranging from 20  $\mu\text{m}$  to 45  $\mu\text{m}$  were prepared in this study. The  $\text{Al}_2\text{O}_3$ -YAP particles were inserted into a Mo mold, which has an outer diameter of 10 mm and an inner diameter of 6 mm. The Mo mold was inserted into a carbon die to avoid Joule heat due to direct current in the Mo mold. The direct current through the carbon die was used to heat the specimen. The carbon die was heated to 2023 K at a heating rate of 1.7 K/s under the given pressures (10, 20, 35, and 50 MPa) and cooled after holding at 2073 K for the given holding time (60 s, 10.8 ks, and 21.6 ks). The microstructures of the  $\text{Al}_2\text{O}_3$ -YAG compacts were observed by scanning electron microscopy (SEM). The volume fraction and size of the porosity of the  $\text{Al}_2\text{O}_3$ -YAG compacts were measured using an image analysis program. The flexural strength of the  $\text{Al}_2\text{O}_3$ -YAG compacts was measured using the three-point bending technique over a span of 10 mm and at a crosshead

speed of 0.1 mm/min. A rectangular specimen of dimensions  $1 \times 2 \times 13 \text{ mm}^3$  was used for the flexural strength test. The surfaces of the specimens were polished with #400 emery paper in a direction perpendicular to the flexural axis.

### 3. Results and Discussions

#### 3.1 Influence of the $\text{Al}_2\text{O}_3$ -YAP eutectic particle size on the $\text{Al}_2\text{O}_3$ -YAG microstructure and flexural strength

Figures 2(a) and (b) show the SEM photographs of the  $\text{Al}_2\text{O}_3$ -YAG compacts produced by melting the  $\text{Al}_2\text{O}_3$ -YAP metastable eutectic particles with diameters ranging from 20  $\mu\text{m}$  to 45  $\mu\text{m}$  and less than 20  $\mu\text{m}$ , respectively. The white and black regions in the SEM photographs indicate the YAG phase and the  $\text{Al}_2\text{O}_3$  phase, respectively. A fine and uniform eutectic structure with a lamellar spacing of 1  $\mu\text{m}$  or less was observed when the  $\text{Al}_2\text{O}_3$ -YAG compact was produced by using the  $\text{Al}_2\text{O}_3$ -YAP metastable eutectic particles with diameters ranging from 20  $\mu\text{m}$  to 45  $\mu\text{m}$ . A eutectic structure in which the lamellar was produced due to coupled growth was recognized in some parts of the compacts. On the other hand, the  $\text{Al}_2\text{O}_3$ -YAG compact produced on using  $\text{Al}_2\text{O}_3$ -YAP particles with diameters less than 20  $\mu\text{m}$  revealed that  $\text{Al}_2\text{O}_3$  phases with a diameter of 2.5  $\mu\text{m}$  were dispersed in the YAG matrix. The morphology was different from that of the  $\text{Al}_2\text{O}_3$ -YAP eutectic particles with diameters in the range of 20  $\mu\text{m}$  to 45  $\mu\text{m}$ .

It was reported that YAG is likely to nucleate at the  $\text{Al}_2\text{O}_3$ /YAP phase boundary, that volume expansion occurred during phase transformation ( $\text{Al}_2\text{O}_3 + 3\text{YAP} = \text{YAG}$ ), and that volume expansion in the solid state suppresses the nucleation of YAG.<sup>6)</sup> Thus, an increase in the three-phase boundary ( $\text{Al}_2\text{O}_3$ /YAP/vacuum) on volume expansion can affect the nucleation and growth of the YAG phase. Consequently, undercooled melt formation can be influenced by the initial  $\text{Al}_2\text{O}_3$ -YAP particle size. In order to clarify the reason why the initial  $\text{Al}_2\text{O}_3$ -YAP particle size resulted in different  $\text{Al}_2\text{O}_3$ -YAG eutectic microstructures, it is important to investigate this phenomenon from the viewpoint of the crystallographic orientation distribution and grain size distribution in the  $\text{Al}_2\text{O}_3$ -YAG eutectic structure.

In the case of the  $\text{Al}_2\text{O}_3$ -YAP metastable eutectic particles with diameters ranging from 20  $\mu\text{m}$  to 45  $\mu\text{m}$  and less than 20  $\mu\text{m}$ , the mean diameters of the porosities were 9  $\mu\text{m}$  and 4  $\mu\text{m}$ , respectively, while the volume fractions of the

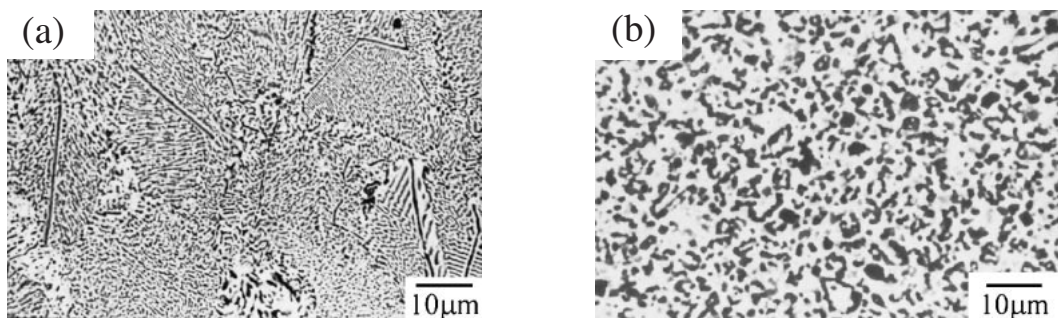


Fig. 2 SEM photographs of the  $\text{Al}_2\text{O}_3$ -YAG compacts ( $\text{Al}_2\text{O}_3$ -23.5 mol%  $\text{Y}_2\text{O}_3$ ) produced by the  $\text{Al}_2\text{O}_3$ -YAP particles with diameters ranging (a) from 20  $\mu\text{m}$  to 45  $\mu\text{m}$  and (b) less than 20  $\mu\text{m}$ .

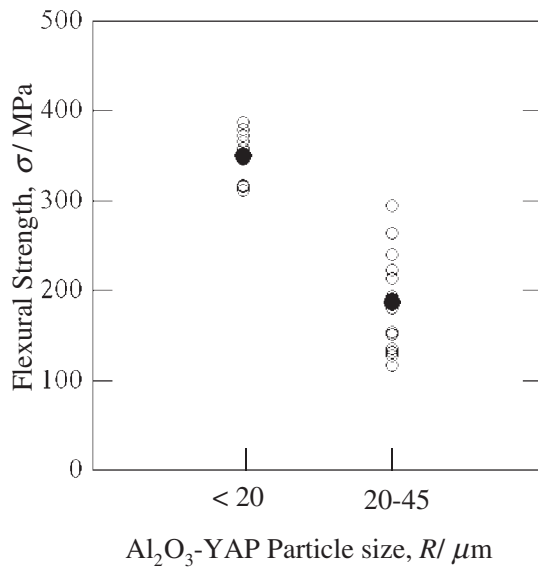


Fig. 3 Flexural strength of the  $\text{Al}_2\text{O}_3$ -YAG compacts ( $\text{Al}_2\text{O}_3$ -23.5 mol% $\text{Y}_2\text{O}_3$ ) produced by the  $\text{Al}_2\text{O}_3$ -YAG particles with diameters ranging from 20  $\mu\text{m}$  to 45  $\mu\text{m}$  and less than 20  $\mu\text{m}$ . The open and closed circles indicate the measured and average values of the flexural strength, respectively.

porosities were 3% and 2%, respectively. The use of finer  $\text{Al}_2\text{O}_3$ -YAG metastable eutectic particles resulted in a reduction in the size of the porosities.

The flexural strengths of the  $\text{Al}_2\text{O}_3$ -YAG compacts produced from the  $\text{Al}_2\text{O}_3$ -YAG eutectic particles with diameters ranging from 20  $\mu\text{m}$  to 45  $\mu\text{m}$  and less than 20  $\mu\text{m}$  are shown in Fig. 3. The average values of the flexural strength of the compacts produced by using  $\text{Al}_2\text{O}_3$ -YAG eutectic particles with diameters ranging from 20  $\mu\text{m}$  to 45  $\mu\text{m}$  and less than 20  $\mu\text{m}$  were 187 MPa and 339 MPa, respectively. As compared to the  $\text{Al}_2\text{O}_3$ -YAG compact produced from  $\text{Al}_2\text{O}_3$ -YAG particles with diameters ranging from 20  $\mu\text{m}$  to 45  $\mu\text{m}$ , the  $\text{Al}_2\text{O}_3$ -YAG compact produced from the  $\text{Al}_2\text{O}_3$ -YAG eutectic particles with diameters less than 20  $\mu\text{m}$  exhibited a higher flexural strength and lower scatter in the measurement of the flexural strength. This small scatter is due to the smaller porosity size.

The  $\text{Al}_2\text{O}_3$ -YAG compact produced from  $\text{Al}_2\text{O}_3$ -YAG eutectic particles with diameters less than 20  $\mu\text{m}$  exhibits a lower fraction of porosity and higher strength in spite of the coarse eutectic structure. Thus, it is concluded that the  $\text{Al}_2\text{O}_3$ -YAG eutectic particles with diameters less than 20  $\mu\text{m}$  are suitable for producing a dense  $\text{Al}_2\text{O}_3$ -YAG compact with a relatively higher flexural strength. In the following experiments,  $\text{Al}_2\text{O}_3$ -YAG metastable eutectic particles with diameters less than 20  $\mu\text{m}$  size were chosen as the starting materials.

### 3.2 Influence of forming pressure on the $\text{Al}_2\text{O}_3$ -YAG microstructure

In order to investigate the influence of the forming pressure on the volume fraction of the porosity, the  $\text{Al}_2\text{O}_3$ -YAG compacts were produced under different forming pressures of 0, 10, 20, 35, and 50 MPa. Figure 4 shows the volume fraction of the porosity in the  $\text{Al}_2\text{O}_3$ -YAG compacts as a

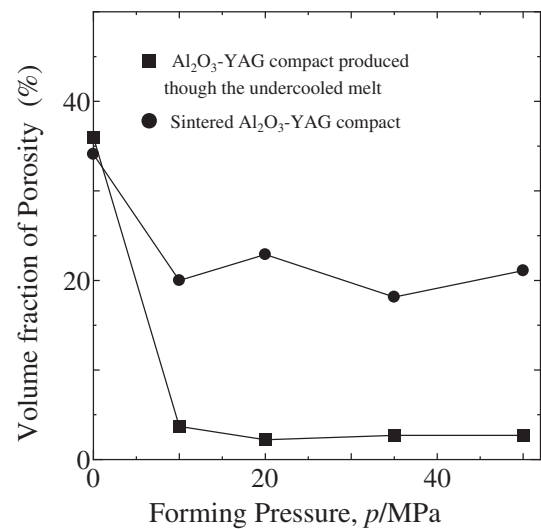


Fig. 4 The forming pressure dependence of volume fraction of the porosity in the  $\text{Al}_2\text{O}_3$ -YAG compact produced using undercooled melt and the sintered  $\text{Al}_2\text{O}_3$ -YAG compact.

function of the forming pressure imposed during shaping. For the purpose of comparison, the volume fraction of the porosity in the sintered  $\text{Al}_2\text{O}_3$ -YAG compacts produced by using  $\text{Al}_2\text{O}_3$  and YAG particles is also presented. The volume fraction of the porosity of both for the  $\text{Al}_2\text{O}_3$ -YAG compacts formed using the undercooled melt shaping and the sintered  $\text{Al}_2\text{O}_3$ -YAG compact for a forming pressure that exceeded 10 MPa was independent of the forming pressure. The volume fraction in the  $\text{Al}_2\text{O}_3$ -YAG compact produced from  $\text{Al}_2\text{O}_3$ -YAG eutectic particles became less than 4%, while the volume fraction of the porosity of the sintered  $\text{Al}_2\text{O}_3$ -YAG compact was approximately 20%. Undercooled melt shaping achieved a high apparent density even under a relatively low pressure such as 10 MPa. The high volume fraction of the porosity is attributed to the 11% volume expansion in the transformation from the  $\text{Al}_2\text{O}_3$ -YAP system to the  $\text{Al}_2\text{O}_3$ -YAG system.<sup>6)</sup>

### 3.3 Influence of holding time on the microstructure and flexural strength

The influences of the holding time at a maximum temperature of 2023 K on the microstructure and mechanical property of the  $\text{Al}_2\text{O}_3$ -YAG compacts were examined. SEM photographs of the  $\text{Al}_2\text{O}_3$ -YAG compacts with a holding time of 60 s, 10.8 ks, and 21.6 ks are shown in Figs. 5 (a), (b), and (c), respectively. The values of the mean diameter of the  $\text{Al}_2\text{O}_3$  grains were 2.5  $\mu\text{m}$  for a holding time of 60 s, 2.7  $\mu\text{m}$  for 10.8 ks, and 4.2  $\mu\text{m}$  for 21.6 ks. The  $\text{Al}_2\text{O}_3$  phase coarsened with increasing holding time. The volume fractions of the porosity at holding times of 60 s, 10.8 ks, and 21.6 ks were 2%, 2%, and 1%, respectively. The volume fraction of the porosity was independent of the holding time. The connections between the initial particles were completed only for a holding time of 60 s.

The average values of the flexural strength at holding times of 60 s, 10.8 ks, and 21.6 ks were 350, 338, and 268 MPa, respectively. The flexural strength reduced with the increase in the holding time. Mah *et al.* reported that the flexural

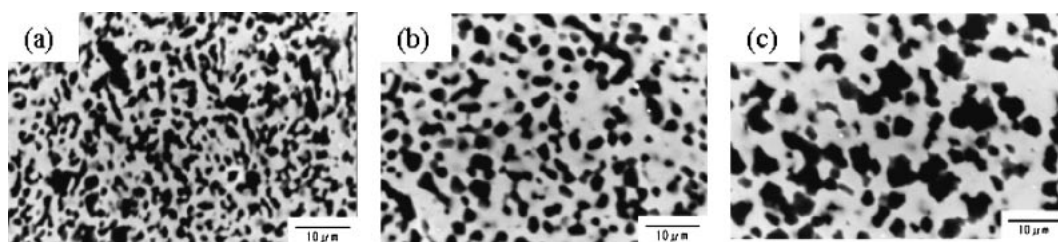


Fig. 5 SEM photographs of the  $\text{Al}_2\text{O}_3$ -YAG compacts kept for holding times of (a) 60 s, (b) 10.8 ks, and (c) 21.6 ks at 2023 K.

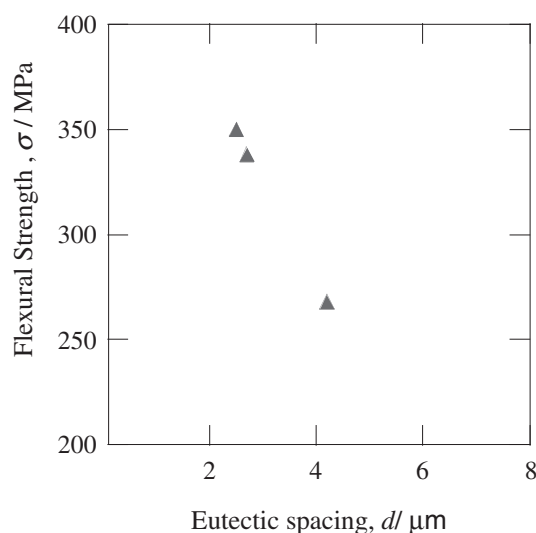


Fig. 6 The flexural strength as a function of eutectic spacing for the  $\text{Al}_2\text{O}_3$ -YAG compacts at holding times of 60 s, 10.8 ks, and 21.6 ks.

strength of the  $\text{Al}_2\text{O}_3$ -YAG system can be determined by the eutectic spacing rather than the grain size.<sup>16,17</sup> Figure 6 shows the flexural strength of the  $\text{Al}_2\text{O}_3$ -YAG compacts at holding times of 60 s, 10.8 ks, and 21.6 ks as a function of the eutectic spacing. The flexural strength has a tendency to depend on the eutectic spacing. Thus, a reduction in the flexural strength is attributable to the increase in the eutectic spacing during holding at the maximum temperature.

Based on these results, the  $\text{Al}_2\text{O}_3$ -YAG compact was immediately formed when undercooled melt was produced at the metastable eutectic temperature. It was not necessary to maintain the compact at the maximum temperature in order to produce a dense compact during undercooled melt shaping.

#### 4. Conclusions

The influences of the initial  $\text{Al}_2\text{O}_3$ -YAP eutectic particle size on the microstructure and mechanical property of  $\text{Al}_2\text{O}_3$ -YAG compact were investigated. Although the  $\text{Al}_2\text{O}_3$ -YAG compact produced from the  $\text{Al}_2\text{O}_3$ -YAP eutectic particles with diameters ranging from  $20\mu\text{m}$  to  $45\mu\text{m}$  had a finer eutectic structure as compared to the compact produced from  $\text{Al}_2\text{O}_3$ -YAP eutectic particles with diameters less than  $20\mu\text{m}$ , utilizing smaller-sized  $\text{Al}_2\text{O}_3$ -YAP eutectic particles provided higher flexural strength. The influence of the forming pressure and holding time at the maximum temperature on the  $\text{Al}_2\text{O}_3$ -YAG microstructure and/or the mechan-

ical property were also examined. The volume fraction of the porosity of the  $\text{Al}_2\text{O}_3$ -YAG compacts was approximately 4% regardless of the forming pressure and holding time. The eutectic spacing increased with the holding time, resulting in a reduction in the flexural strength. In the solidification from the undercooled melt formed by melting the  $\text{Al}_2\text{O}_3$ -YAP eutectic particles with diameters less than  $20\mu\text{m}$ , a dense  $\text{Al}_2\text{O}_3$ -YAG compact was produced under a low forming pressure of 10 MPa and a short holding time of 60 s.

#### Acknowledgement

This work is supported in part by a Grant-in-Aid for Scientific Research. This work is also supported by the 21st Century COE Program from the Ministry of Education, Sports, Culture, Science and Technology of Japan.

#### REFERENCES

- 1) T. Mah and T. A. Parthasarathy: *Ceram. Eng. Sci. Proc.* **11** (1990) 1617–1627.
- 2) Y. Waku, N. Nakagawa, T. Wakamoto, H. Ohtsubo and K. Shimizu: *Nature* **389** (1997) 49–52.
- 3) Y. Waku, N. Nakagawa, T. Wakamoto, H. Ohtsubo, K. Shimizu and Y. Kohtoku: *J. Mater. Sci.* **33** (1998) 1217–1225.
- 4) Y. Waku, N. Nakagawa, T. Wakamoto, H. Ohtsubo, K. Shimizu and Y. Kohtoku: *J. Mater. Sci.* **33** (1998) 4943–4951.
- 5) T. A. Parthasarathy and T. Mah: *J. Am. Ceram. Soc.* **76** (1993) 29–32.
- 6) Randall S. Hay: *J. Am. Ceram. Soc.* **77** (1994) 1473–1485.
- 7) J. L. Caslavsky and D. J. Viehnick: *J. Mater. Sci.* **15** (1980) 1709–1718.
- 8) H. Yasuda, I. Ohnaka, Y. Mizutani and Waku: *Sci. Tech. Adv. Mater.* **2** (2001) 67–71.
- 9) H. Yasuda, I. Ohnaka, Y. Mizutani and Y. Waku: *Proc. M. C. Flemings Symposium TMS.* (2001) 171–176.
- 10) H. Yasuda, T. Mizutani, I. Ohnaka, A. Sugiyama and Y. Waku: *Mater. Trans.* **42** (2001) 2124–2130.
- 11) Y. Mizutani, H. Yasuda, I. Ohnaka, A. Sugiyama, S. Takeshima, M. Kirihaara and Y. Waku: *Mater. Trans.* **43** (2002) 2847–2854.
- 12) Y. Mizutani, H. Yasuda, N. Maeda and Y. Waku: *J. Cryst. Growth.* **244** (2002) 384–392.
- 13) H. Yasuda, Y. Mizutani, I. Ohnaka, A. Sugiyama and T. Morikawa: *J. Am. Ceram. Soc.* **86** (2003) 1818–1820.
- 14) H. Yasuda, I. Ohnaka, Y. Mizutani, A. Sugiyama, T. Morikawa, S. Takeshima, T. Sakimura and Y. Waku: *Sci. Tech. Adv. Mater.* **5** (2004) 207–217.
- 15) H. Yasuda, I. Ohnaka, A. Sugiyama, Y. Mizutani, T. Sakimura, A. Kawaguchi and Y. Waku: *Mater. Sci. Form.* **475–479** (2005) 2709–2712.
- 16) T. Mah, T. A. Parthasarathy and R. J. Kerans: *J. Am. Ceram. Soc.* **83** (2000) 2088–2090.
- 17) T. A. Parthasarathy, T. Mah and L. E. Matson: *J. Ceram. Proc. Res.* **5** (2004) 380–390.